Biochimie 94 (2012) 2297–2307

Contents lists available at SciVerse ScienceDirect

Biochimie

journal homepage: www.elsevier.com/locate/biochi

Research paper

Antineoplastic activity of the DNA methyltransferase inhibitor 5-aza-2′-deoxycytidine in anaplastic large cell lymphoma

Melanie R. Hassler [a,b], Aleksandra Klisaroska [a], Karoline Kollmann [c], Irene Steiner [d], Martin Bilban [e], Ana-Iris Schiefer [a], Veronika Sexl [c], Gerda Egger [a,*]

[a] Clinical Institute of Pathology, Medical University of Vienna, Waehringer Guertel 18-20, 1090 Vienna, Austria
[b] Department of Internal Medicine I, Medical University of Vienna, Vienna, Austria
[c] Institute of Pharmacology and Toxicology, Veterinary University Vienna, Vienna, Austria
[d] Center for Medical Statistics, Informatics, and Intelligent Systems, Section for Medical Statistics, Medical University of Vienna, Vienna, Austria
[e] Department of Laboratory Medicine, Medical University of Vienna, Vienna, Austria

ARTICLE INFO

Article history:
Received 16 February 2012
Accepted 31 May 2012
Available online 9 June 2012

Keywords:
DNA methyltransferase inhibitor
5-Aza-2′-deoxycytidine
Decitabine
Anaplastic large cell lymphoma
NPM-ALK
T-cell lymphoma

ABSTRACT

DNA methylation is an epigenetic mechanism establishing long-term gene silencing during development and cell commitment, which is maintained in subsequent cell generations. Aberrant DNA methylation is found at gene promoters in most cancers and can lead to silencing of tumor suppressor genes. The DNA methyltransferase inhibitor 5-aza-2′-deoxycytidine (5-aza-CdR) is able to reactivate genes silenced by DNA methylation and has been shown to be a very potent epigenetic drug in several hematological malignancies. In this report, we demonstrate that 5-aza-CdR exhibits high antineoplastic activity against anaplastic large cell lymphoma (ALCL), a rare CD30 positive non-Hodgkin lymphoma of T-cell origin. Low dose treatment of ALCL cell lines and xenografted tumors causes apoptosis and cell cycle arrest *in vitro* and *in vivo*. This is also reflected in genome-wide expression analyses, where genes related to apoptosis and cell death are amongst the most affected targets of 5-aza-CdR. Furthermore, we observed demethylation and re-expression of $p16^{INK4A}$ after drug administration and senescence associated β-galactosidase activity. Thus, our data provide evidence that 5-aza-CdR is highly efficient against ALCL and warrants further clinical evaluation for future therapeutic use.

© 2012 Elsevier Masson SAS. Open access under CC BY-NC-ND license.

1. Introduction

DNA methylation is an epigenetic regulatory mechanism, which occurs at cytosine residues mainly in CpG dinucleotides and ensures long-term silencing of inactive genomic regions [1]. In cancer, DNA methylation is decreased on a genome-wide scale, but it is also directed to CpG islands, which are normally unmethylated and may account for silencing of tumor suppressor genes [2]. Epigenetic drugs such as DNA methyltransferase inhibitors 5-azacytidine (5-aza-CR, Vidaza®) or the more stable 5-aza-2′-deoxycytidine (5-aza-CdR, decitabine, Dacogen®) are used to reverse DNA methylation in order to induce the re-expression of silent genes [3,4]. Mechanistically, 5-aza-CR and 5-aza-CdR, which are nucleoside analogs, work via incorporation into DNA of actively proliferating cells. Upon incorporation, they irreversibly trap DNA methyltransferases (DNMTs) by forming covalent complexes [5,6]. Thereby, they inhibit propagation of DNA methylation during each round of replication at low doses, whereas at high doses cytotoxic side effects can occur [7]. 5-Aza-CdR has been approved by the Food and Drug Administration (FDA) for the treatment of myelodysplastic syndrome and low dose administration of 5-aza-CdR has been tested in promising clinical trials of hematological malignancies such as CML and AML, whereas less striking results have been observed for solid tumors [8–11].

The systemic anaplastic large cell lymphoma (ALCL) is a rare hematological malignancy of T-cell origin, with peak incidences in children/young adults and in people over 60 years of age [12]. It is classified as a CD30 positive non-Hodgkin lymphoma and can be histopathologically characterized based on the appearance of large

Abbreviations: ALCL, anaplastic large cell lymphoma; ALK, anaplastic lymphoma kinase; AML, acute myeloid leukemia; 5-Aza-CdR, 5-aza-2′-deoxycytidine; CML, chronic myeloid leukemia; COBRA, Combined Bisulfite Restriction Analysis; DNMT1, DNA methyltransferase 1; HE, hematoxylin and eosin; JAK/STAT, Janus kinase/signal transducer and activator of transcription; MAPK, mitogen-activated protein kinase; M.SssI, CpG methyltransferase; NPM-ALK, nucleophosmin-anaplastic lymphoma kinase; PBMCs, peripheral blood mononuclear cells; PI3-K/AKT, phosphatidylinositol-3 kinase/AKT; PLCγ, phospholipase Cγ.

* Corresponding author. Tel.: +43 1 40400 6389; fax: +43 1 40400 5179.
E-mail address: gerda.egger@meduniwien.ac.at (G. Egger).

0300-9084 © 2012 Elsevier Masson SAS. Open access under CC BY-NC-ND license.
http://dx.doi.org/10.1016/j.biochi.2012.05.029

pleomorphic hallmark cells. Frequently, ALCLs carry a chromosomal translocation (t(2; 5)(p23; q35)), which results in the generation of the oncogenic fusion protein NPM-ALK (nucleophosmin-anaplastic lymphoma kinase) [13–15]. The fusion protein acts as a constitutive active kinase and aberrantly activates multiple cellular pathways including JAK/STAT (Janus kinase/signal transducer and activator of transcription), PI3-K/AKT (phosphatidylinositol-3 kinase/AKT), MAPKs (mitogen-activated protein kinases), and PLCγ (phospholipase Cγ), which lead to enhanced proliferation and cell transformation [16–18].

DNA hypermethylation in ALCL was shown for a handful of genes including the tumor suppressor $p16^{INK4A}$ and genes involved in T-cell receptor signaling and T-cell identity [19–23]. Interestingly, the inhibition of DNMT1 by DNMT1 antisense oligonucleotides was capable to suppress activation of STAT3, providing a molecular rationale to target DNA methylation by treatment with epigenetic drugs in the disease [24].

Currently, the therapy for ALCL consists of standard chemotherapy, however, the efficiency of treatment schemes can be limited due to the occurrence of relapses and development of drug resistance when certain risk factors are present [25]. Thus, alternative therapy options need to be considered.

In the current study, we evaluated the *in vitro* and *in vivo* effects of the DNMT inhibitor 5-aza-CdR on ALCL with a focus on ALK positive (ALK+) lymphoma cells. This study was prompted by the finding that both ALK+ and ALK negative (ALK− ALCL cells display high expression levels of the main 5-aza-CdR) target DNMT1. Low dose drug treatments resulted in increased apoptosis, cell cycle arrest and a senescence-like phenotype as indicated by higher β-galactosidase activity and demethylation and re-expression of $p16^{INK4A}$ after drug administration. Global gene expression analysis revealed cell death and apoptosis as central processes affected by 5-aza-CdR in KARPAS-299 cells, and our top de-regulated targets included cancer testis antigens, genes involved in cell adhesion and migration and in immune response. We conclude − based on our *in vitro* and *in vivo* data − that 5-aza-CdR effectively blocks tumor progression in ALCL and might represent a promising treatment option for epigenetic therapy or combination with standard chemotherapy in this disease entity.

2. Materials and methods

2.1. Human ALK+ and ALK− ALCL patient samples

Archived formalin fixed paraffin embedded (FFPE) tumors from ALK+ and ALK− ALCL patients and lymph node controls were obtained blinded and randomized from the Institute of Clinical Pathology at the Medical University of Vienna in accordance with the declaration of Helsinki and Austrian legislature.

2.2. Immunohistochemistry

Tissue arrays containing 30 ALK+ samples, 5 ALK− samples and 7 lymph nodes were dewaxed and rehydrated using standard procedures. Epitopes were retrieved by heat-treatment in citrate buffer (DAKO). Endogenous peroxidase was blocked with 3% H_2O_2 (Gatt–Koller) for 10 min. Sections were blocked with Avidin/Biotin block (Vector) and Superblock (IDLabs). Slides were incubated with primary antibody against DNMT1 (abcam, ab13537) or CD30 (DAKO, M0751) diluted in 1% PBS/BSA over night at 4 °C, followed by incubation with secondary antibody and Streptavidin HRP (IDLabs). Arrays were stained with AEC (ID-Labs) for DNMT1 or DAB (Thermo Scientific) for CD30 and counterstained with hematoxylin (Merck). Pictures were taken with an Olympus Vanux AHBT3 microscope and the ProgRes C12 program.

2.3. Cell culture

2.3.1. Cell lines and chemicals

KARPAS-299 and SR-786 (ALK+ ALCL) and MAC-2A (ALK− ALCL) human cell lines were grown in RPMI 1640 medium (GIBCO) containing 10% FBS (fetal bovine serum) and 1% penicillin/streptomycin at 37 °C in an atmosphere of 5% CO_2 and 95% room air. 5-Aza-2′-deoxycytidine (5-aza-CdR) was obtained from Sigma–Aldrich, dissolved in PBS (GIBCO) to a concentration of 1 mM and stored at −80 °C until use.

For population doubling analysis, MAC-2A, KARPAS-299 and SR-786 cell lines were seeded in six-well plates (BD Biosciences) at a density of 5×10^5 cells/ml in RPMI medium. 5-Aza-CdR was added either once (d0) or every other day (d0, d2, d4) to a final concentration of 1 μM and PBS was added to control cells. After 2, 4 and 6 days cells were counted using a CASY cell counter (Schaerfe System), centrifuged and diluted to 5×10^5 cells/ml in fresh RPMI medium. Population doublings between measurements were calculated according to the formula: population doublings = ln (concentration counted/concentration seeded) and overall population doublings were calculated by summing up preceding values.

2.3.2. Cell cycle analysis

For cell cycle analysis, KARPAS-299 cells were incubated for 24 h with 1 μM of 5-aza-CdR in RPMI and grown for 4 days in fresh RPMI only. Then, 10^5–10^6 cells were suspended in 500 μl PI-buffer (0.1% Na–citrat dihydrate (Sigma), 0.1% Triton X-100 (Sigma), 0.1% RNAse (DNAse free, Sigma) in PBS). Propidium–iodide (ROTH, dissolved in PBS) was added to a concentration of 10 μg/ml and the cells were incubated for 30 min at 37 °C. The analysis was performed on a BD FACSCanto II flow cytometer using the BD FACS Diva Software. Three independent samples of 5-aza-CdR treated and PBS controls were analysed. Descriptive statistics for analysis are reported as mean ± SEM.

2.3.3. Methylation analysis by Combined Bisulfite Restriction Analysis (COBRA)

For methylation analysis, 1×10^6 KARPAS-299 and MAC-2A cells were incubated with 0, 1 and 10 μM of 5-aza-CdR in RPMI, the medium was changed after 24 h and then cells were grown for 4 days in RPMI only. Cells were centrifuged, washed and dissolved in genomic DNA isolation buffer (0.4 M NaCl, 0.2% SDS, 0.1 M Tris pH 8.3, 5 mM EDTA). After RNAse A (20 μg/ml, Invitrogen) and Proteinase K (500 μg/ml, Invitrogen) digestion at 55 °C over night, phenol/chloroform extraction was performed and the DNA was precipitated with 1×vol. of isopropanol. The DNA pellet was washed with 75% ethanol, dried at room temperature, dissolved in sterile water and incubated at 37 °C until completely dissolved. DNA concentration was measured on a Nanodrop 2000 (Thermo Scientific). To obtain a methylated control, 20 μg of DNA isolated from PBMCs were methylated by M.SssI (NEB, 80U) *in vitro* for 6 h at 37 °C with 160 μM S-adenosylmethionine (NEB) and purified by phenol/chloroform extraction as described above.1 μg of DNA was bisulfite-converted with the EZ DNA Methylation™ Kit (Zymo Research) according to the manufacturer's protocol. Over night conversion was carried out in a thermocycler at 95 °C for 30 s, 50 °C for 60 min (16 cycles). For COBRA-PCR, a PCR reaction contained 2.5 μl 10× AmpliTaqGold Buffer (Applied Biosynthesis), 2.5 μl $MgCl_2$ (Applied Biosynthesis), 0.5 μl dNTPs (Invitrogen), 1 μl 10 mM $p16^{INK4A}$ primers (forward + reverse), 0.125 μl AmpliTaqGold Polymerase (Applied Biosynthesis), 16.5 μl H_2O and 2 μl of bisulfite-converted DNA. Primers for amplification of bisulfite converted DNA were designed using the SEQUENOM EpiDesigner program (http://www.epidesigner.com/). Primer sequences used were

p16fw: 5′-GTA GGT GGG GAG GAG TTT AGT TT-3′ and p16rv: 5′-CCT ATC CCT CAA ATC CTC TAA AAA-3′ (PCR product size: 220 bp, restriction by TaqI: restriction fragments 150 bp and 70 bp). Restriction of the PCR product for the $p16^{INK4A}$ promoter was performed for 3 h at 65 °C by incubation with TaqI (New England Bio Labs) (15 μl PCR product, 2 μl 10× NEB buffer 4, 2 μl 10× BSA, 0.5 μl TaqI, 0.5 μl H_2O). Restriction fragments were analyzed on an Agilent 2100 Bioanalyzer platform using the Agilent DNA chip 1000 series. Chip preparation was carried out according to the manufacturer's protocol. 1 μl of the restriction product was loaded onto the chip. For quantification of methylated and unmethylated fragments, the areas under the methylated and unmethylated peaks in electropherograms were measured by Agilent software and the percentage of methylated or unmethylated fragments in relation to total peak areas was calculated.

2.3.4. RNA extraction, gene expression profiling and quantitative reverse transcription PCR (qRT–PCR)

For gene expression analysis, 1×10^6 KARPAS-299 cells were incubated with 1 μM of 5-aza-CdR or PBS for 24 h in RPMI, the medium was changed to RPMI only and the cells were grown for 4 days. Then, cells were centrifuged, washed and RNA was extracted using the RNAeasy Mini kit (Qiagen) according to protocol. RNA concentration was measured on the Nanodrop 2000 (Thermo Scientific) and RNA quality was determined on an Agilent 2100 Bioanalyzer platform. Total RNA (200 ng) was then used for GeneChip analysis. Preparation of terminal-labeled cDNA, hybridization to genome-wide human Gene Level 1.0 ST GeneChips (Affymetrix, Santa Clara, CA, USA) and scanning of the arrays were carried out according to manufacturer's protocols https://www.affymetrix.com.

For qRT–PCR quantification, 1 μg of RNA was used as template for random hexamer cDNA synthesis (Invitrogen) using Superscript (200 U/μl) (Invitrogen) according to supplier's protocol. qRT–PCR was performed with FASTAKapa Mastermix (Peqlab biotechnologies) on a Biorad cycler, 2 μl of cDNA were used per sample. GAPDH was used for normalisation. RT-primer sequences for $p16^{INK4A}$ were fw: 5′-GGG TCG GGT AGA GGA GGT G-3′ and and rv: 5′-ACG GGT CGG GTG AGA GTG-3′ and for GAPDH fw: 5′-GGT GGT CTC CTC TGA CTT CAA CA-3′ and rv: 5′-GTT GCT GTA GCC AAA TTC GTT GT-3′. Three independent samples were processed. RT-primer sequences for confirmation of array data were: MAGE2B fw: 5′-CAG GGG TGA ATT CTC AGG AC-3′, rv: 5′-GGC CTC TTC TTC CTC TGC TT-3′, MMP13 fw: 5′-GGT TCC TGA TGT GGG TGA AT-3′, rv: 5′-CAA TGC CAT CGT GAA GTC TG-3′, SPARC fw: 5′-CAG AAC CAC CAC TGC AAA CA-3′, rv: 5′-AAG TGG CAG GAA GAG TCG AA-3′, TGFB1 fw: 5′-GAG CCT GAG GCC GAC TAC TA-3′, rv: 5′-GGG TTC AGG TAC CGC TTC TC-3′, TNFAIP2 fw: 5′-CTG GAC TTG GGC TCA CAG AT-3′, rv: 5′-CAG GCA GTT GTT GAT GTT GG-3′and CXC11 fw: 5′-GCA GCA AAG CTG AAGTAGCA-3′, rv: 5′-ATG CAA AGA CAG CGT CCT CT-3′.

2.3.5. Bioinformatic analysis of global gene expression

Statistical analyses were conducted with the bioconductor packages Affy and limma [26–28]. Quality assessment was done by boxplots, histograms and correlation plots. We normalized the data using the robust multi-array average (RMA) expression measure. Before starting the analyses, we filtered the data. Probes were included in the analysis if the IQR over all chips was greater than 0.5 and if at least two of the chips showed intensity above the cut point of log 2 (100). After filtering the data, 4901 of 32,321 probes remained. For comparison of the chips we calculated moderated t-statistics (bioconductor package limma) and corrected for multiple testing by Benjamini–Hochberg correction. The analysis was repeated without filtering the data and including only genes that are described in Gius [29] and Carén [30], respectively. In total, 943 genes were selected for the statistical analysis. Thereof, 725 probes could be assigned to a gene symbol. For pathway analysis, we used ingenuity pathway analysis (IPA) software (http://www.ingenuity.com/). For all analyses, the significance level has been set to 0.05.

2.3.6. Dose–response curve

For dose–response curves, 5×10^5 cells/ml were incubated with 0.01, 0.03, 0.1, 0.3, 1, 3 and 10 μM of 5-aza-CdR for 24 h in RPMI, the medium was changed and cells were grown for 4 days. Then, 5×10^4 cells of each concentration were plated in 96 well dishes in triplicates, 0.1 μCi [^{3}H]–thymidine/well (Perkin–Elmer) were added and cells were incubated for another 12 h. After 12 h of incubation, [^{3}H]-incorporation was measured with Ultima Gold MV scintillation fluid (Packard Instruments) by a scintillation counter. The dose–response curve (log *c* vs counts per minute/CPM) was calculated by assuming a sigmoid dose–response curve (variable slope).

2.3.7. Protein extraction and Western Blot

Human peripheral blood mononuclear cells (PBMCs) were isolated from 50 ml of whole blood obtained from a healthy female volunteer using Lymphoprep solution (Axis-shield) according to manufacturer's protocol.

PBMC, MAC-2A, KARPAS-299 and SR-786 cell pellets were dissolved in Hunt buffer (20 mM Tris pH 8, 100 mM NaCl, 1 mM EDTA, 0.5% NP-40, protease inhibitor (Roche)), frozen in liquid nitrogen, put at 37 °C to thaw, then frozen again and put on ice until completely thawed. The solution was centrifuged for 10 min at 4 °C and protein concentration of the supernatant was measured using the Nanodrop 2000 (Thermo Scientific). Samples were diluted with 2× protein loading dye (100 mM Tris–HCl pH 6.8, 200 mM DTT, 4% SDS, 20% Glycerin, bromophenolblue), heated for 5 min at 95 °C and loaded onto SDS–PAGE (5–15%) gradient gels. 50 μg of protein were loaded per lane. The gels were transferred onto nitrocellulose membranes (wet o/n transfer at 25V, Biorad). Membranes were blocked in blocking solution (5% milk powder, 0.02% NaN_3) (Sigma) in TBS-T (TBS containing 1% Triton-X100, Sigma) for 1 h at RT and incubated with primary antibody against DNMT1 (abcam, ab13537), ALK1 (Zymed, 51-3900) or CD30 (DAKO, M0751) (all 1:1000 in blocking solution), o/n at 4 °C. After washing, incubation with secondary antibody (1:10,000) for 1 h at RT and again washing with TBS-T, the membranes were incubated with chemoluminiscent solution ECL plus (GE Healthcare) and signals were detected using the Lumi Analyst (Roche Applied Science). The same membranes were incubated with β-Actin antibody (Cell signaling, #4967) (1:1000 in blocking solution) as loading control as described above.

2.3.8. β-Galactosidase staining

KARPAS-299 cells were incubated for 24 h with 1 μM of 5-aza-CdR in RPMI and grown for 4 days in fresh RPMI only. Then, 10^4–10^5 cells were centrifuged onto glass slides, washed in PBS and fixed and stained for β-galactosidase with the senescence β-galactosidase staining kit (cell signaling, #9860) according to protocol. Nuclei were counterstained with nuclear fast red.

2.4. Xenograft

2.4.1. Animals

For xenografts, *NOD.CB17-Prkdc-scid/NCrHsd* (NOD/SCID, Harlan Laboratories) mice were used in collaboration with the Pharmacology Department of the Medical University of Vienna. All animal experiments were carried out in accordance with the Austrian Act on Animal Experimentation 1988 (GZ 66.009/139-II/10b/2009). The mice were kept in a controlled environment of light, humidity and

temperature. Food and water were provided every day. KARPAS-299 human cells were grown as described above, dissolved in sterile PBS to a concentration of 1×10^7 cells/ml and inoculated subcutaneously (1×10^6 cells/injection) into the right and left flanks of the mice. Tumor range was followed measuring tumor length and tumor width with a calliper.

2.4.2. Treatment procedure

Mice weighed approximately 25 g at the beginning of the therapy. 5-Aza-CdR was dissolved in sterile PBS and was administered intraperitoneally (i.p.). Each mouse received 2.5 mg/kg/mouse per treatment. Control mice were administered 100 µl of sterile PBS. Therapies were adjusted regarding start and duration of the treatment in order to obtain optimal treatment procedures. In schedule A (Supplementary Fig. S2A), three mice were treated with 5-aza-CdR 11 days after inoculation, when tumor size was approximately 1 cm^2. The control group contained two mice. The mice received 5-aza-CdR or PBS every day for eight days. In the schedule B, two mice were treated with 5-aza-CdR three days after inoculation and three mice five days after inoculation when tumors were not or just palpable. 5-Aza-CdR was administered every other day for five times to each mouse. The control group contained two mice.

2.4.3. Cell cycle analysis

For cell cycle analysis, 100 mg of freshly isolated tumor tissue were pressed through a 100 µm cell strainer (BD Biosciences) and the cell suspension was propidium–iodide stained and further processed as described above for cell lines. Descriptive statistics for analysis are reported as mean ± SEM.

2.4.4. Immunohistochemistry

Tumor tissue was cross-linked in 4% paraformaldehyde, dehydrated in ethanol and embedded in paraffin. 3 µM sections were cut, attached to slides, dewaxed and rehydrated. Epitopes were retrieved by heat-treatment in citrate buffer (DAKO) and slides were processed as described above for tissue arrays. Sections were incubated with primary antibody against Ki-67 (Novocastra, NCL-KI67-P) or Caspase3 (Cell signaling, #9661) diluted in 1% PBS/BSA over night at 4 °C. Slides were stained with AEC (ID-Labs) and counterstained with hematoxylin (Merck). Hematoxilin and eosin staining was done using an automatic tissue stainer (Medite).

2.4.5. Protein extraction and Western Blot

For protein extraction from tumors, tumor tissue was dounced 10–15 times in lysis buffer (20 mM Tris pH 8, 100 mM NaCl, 1 mM EDTA, 0.5% NP-40, protease inhibitor (Roche)). The homogenate was frozen in liquid nitrogen, put on ice to thaw and centrifuged at 4 °C. Protein concentration in the supernatant was measured on a Nanodrop 2000 (Thermo Scientific). SDS–PAGE and Western Blot were carried out as described above for cell lines.

2.4.6. Statistics

Results are shown as means ± SEM. The significance of the differences between mean values was determined by one-way ANOVA followed by pair wise comparisons to the control group using unpaired *t*-tests.

3. Results

3.1. High expression levels of DNMT1 in human ALCL cell lines and primary tumors

DNMT1 is essential for development and the proliferation of cancer cells [31–33]. As DNMTs might represent a therapeutic window for epigenetic therapy, we were interested to investigate DNMT1 expression in ALCL cells. Western Blot analysis revealed high DNMT1 levels in ALK+ cell lines KARPAS-299 and SR-786 as well as in the ALK− cell line MAC-2A. In contrast, we failed to detect DNMT1 expression in normal peripheral blood mononuclear cells (PBMCs) isolated from a healthy donor (Fig. 1A). The findings prompted us to further investigate DNMT1 expression in human patient samples. A tissue array consisting of 30 formalin fixed paraffin embedded (FFPE) tumors from ALK+ ALCL patients, 5

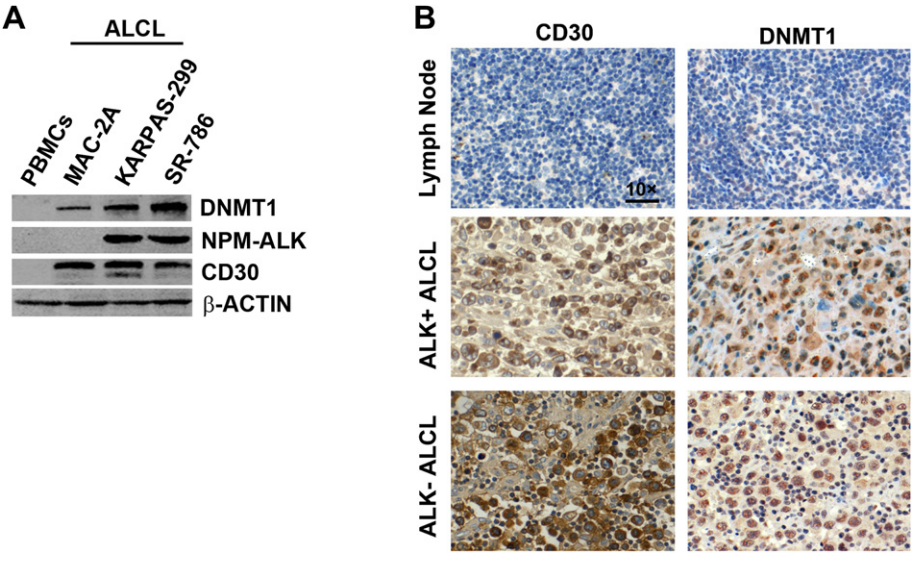

Fig. 1. Enhanced DNMT1 expression is detected in human ALCL cell lines and patient samples. A. DNMT1 is overexpressed in human ALCL cell lines compared to normal peripheral blood mononuclear cells (PBMCs). Proteins were extracted from PBMCs, ALK− ALCL cell line MAC-2A and ALK+ ALCL cell lines KARPAS-299 and SR-786 and analysed by Western Blot as described in materials and methods. B. DNMT1 is expressed in human ALK+ ALCL tumor cells, but not in healthy lymph nodes. Immunohistochemical staining against DNMT1 was performed on a human ALCL tissue array containing 30 ALK+ and 5 ALK− ALCL patient samples and 7 normal lymph nodes as controls. One representative lymph node, one representative ALK+ and one ALK− ALCL sample are shown. CD30 is used as diagnostic marker for ALCL. Note the typical abnormal anaplastic large cell morphology of CD30 positive cells compared to healthy lymphocytes.

tumors from ALK− ALCL patients and 7 lymph nodes from healthy individuals as controls was manufactured and stained for DNMT1 expression. High DNMT1 expression was found in all CD30 positive ALCL cells, whereas only minor DNMT1 expression was detected in control lymph nodes (Fig. 1B).

3.2. 5-Aza-2′-deoxycytidine inhibits proliferation of ALCL cells

5-Aza-2′-deoxycytidine (5-aza-CdR) is a potent DNMT inhibitor and has recently been approved by the FDA [4]. The high levels of DNMT1 expression detected in ALCL prompted us to study the effects of this drug and to test whether these cells are particularly sensitive to inhibition of DNA methylation. Thus, we incubated ALK+ KARPAS-299 and SR-786 and ALK− MAC-2A cells with 1 μM 5-aza-CdR for six days, counted cells and calculated overall population doublings for this period. 5-Aza-CdR was added either once at the beginning of the treatment (d0) or every second day (d0, d2, d4) when the growth medium was changed. After four days in culture, a clear decrease in population doublings could be observed for all three cell lines upon treatment with 5-aza-CdR, irrespective whether the drug had been applied once or multiple times (Fig. 2A and Supplementary Fig. S1). Cell cycle analysis of KARPAS-299 cells after 4 days showed an increase of 5-aza-CdR treated cells in G1 phase compared to PBS treated control cells (70.4% ± 0.7% vs 63.8% ± 1.9%) and a decrease of 5-aza-CdR treated cells in S phase (25.9% ± 0.6% vs 34.7% ± 1.9%). In addition, the viability of the cells was impaired, and 5-aza-CdR treated cells showed a significant increase of apoptotic cells when compared to mock treated cells (33.7% ± 0.8% in 5-aza-CdR treated versus 23.0% ± 1.4% in control cells) (Fig. 2B). The EC_{50} value was determined by measuring [^{3}H]−thymidine uptake in KARPAS-299 cells after incubation with increasing 5-aza-CdR concentrations. It was calculated by analysing the resulting dose−response curve (Fig. 2C). The EC_{50} value was 0.49 μM, which is in a similar range to the ones observed in common AML cell lines [34].

3.3. 5-Aza-CdR induces demethylation and re-expression of the tumor suppressor $p16^{INK4A}$

5-Aza-CdR inhibits propagation of DNA methylation and induces re-expression of methylated genes [35,36]. Some of these methylated genes play a crucial role in controlling cell cycle progression, i.e tumor suppressor $p16^{INK4A}$ (cyclin-dependent kinase inhibitor 2A CDKN2A). $p16^{INK4}$, which is controlling cell cycle progression through the G1 phase, is capable to induce senescence and has been reported to be methylated in some ALCL tumor cells [19]. When we analysed the $p16^{INK4A}$ promoter methylation status by COBRA, we found that the promoter of $p16^{INK4A}$ was methylated in KARPAS-299 cells and methylation decreased upon 5-aza-CdR treatment in a dose dependent manner (Fig. 3A).

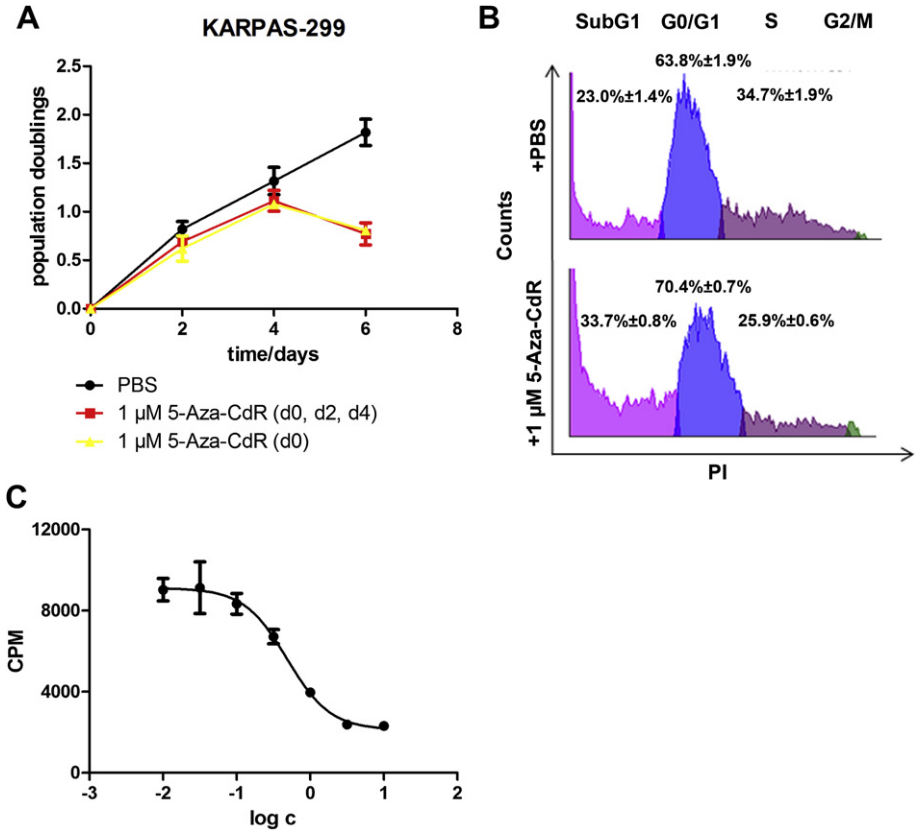

Fig. 2. 5-Aza-CdR inhibits ALCL cell proliferation *in vitro*. A. Treatment of ALCL cell lines with 5-aza-CdR leads to a decrease in population doublings after 4 days in culture. 1 μM of 5-aza-CdR was either administered once (d0) or every other day (d0, d2, d4) to the ALK+ ALCL cell line KARPAS-299. Cells were counted using a CASY cell counter and population doublings were calculated as described in materials and methods. Values are means ± SD. Each value is the mean of three replicates. B. Cell cycle analysis of 5-aza-CdR treated KARPAS-299 cells compared to control cells shows an increase in G1, a decrease in S and an increase in apoptotic cells. KARPAS-299 cells were treated with 1 μM 5-aza-CdR (d0) or PBS for 4 day as described in A. Percentages are means ± SEM. The analysis was performed with three replicates. Two representative FACS graphs are shown. C. Dose−response curve for KARPAS-299 cells treated with different 5-aza-CdR concentrations. The EC_{50} value for 5-aza-CdR treated KARPAS-299 cells is 0.49 μM. 5 × 105 cells/ml were incubated with 0.01, 0.03, 0.1, 0.3, 1, 3 and 10 μM of 5-aza-CdR for 24 h, the medium was changed and cells were grown for four days. Then, 5 × 105 cells of each concentration were plated in 96 well dishes in triplicates and incubated with 0.1 μCi [^{3}H]−thymidine/well for 12 h [^{3}H]-incorporation was measured by liquid scintillation counting. For analysis, a sigmoid dose−response curve (variable slope) was assumed. Log concentration was plotted versus counts per minute (CPM).

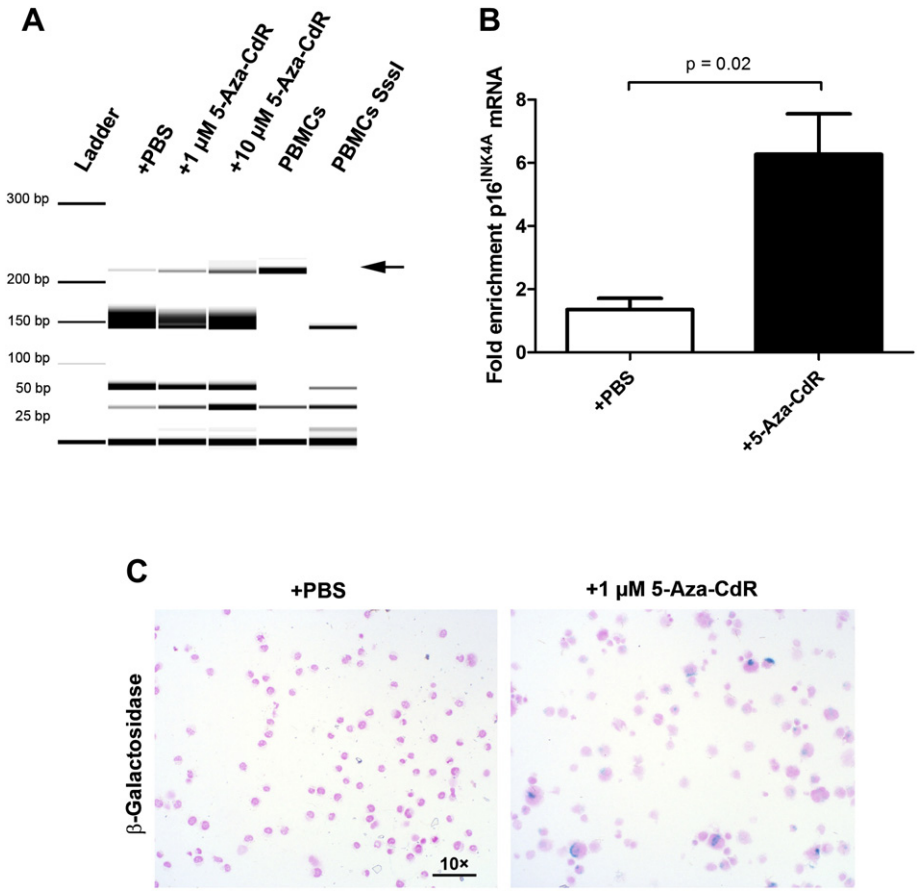

Fig. 3. 5-Aza-CdR treatment leads to demethylation and re-expression of the tumor suppressor $p16^{INK4A}$ and induces cellular senescence. A. $p16^{INK4A}$ promoter methylation decreases upon treatment with increasing 5-aza-CdR concentrations. 1×10^6 KARPAS-299 cells were incubated with 0, 1 and 10 µM of 5-aza-CdR, the medium was changed after 24 h and then cells were grown for 4 days. DNA was extracted from cells and bisulfite converted and Combined Bisulfite Restriction Analysis (COBRA) was performed to analyse the methylation status of the $p16^{INK4A}$ promoter as described in materials and methods. Restriction fragments were analysed using the Agilent 2100 Bioanalyzer platform. Note the dose-dependent increase of the unmethylated fragment at 220 bp indicated by the arrow. B. $p16^{INK4A}$ mRNA increases in the 5-aza-CdR treated cell line KARPAS-299 compared to mock treated controls. RNA was isolated from 1 µM 5-aza-CdR treated KARPAS-299 cells as described in A. $p16^{INK4A}$ expression was analysed by quantitative RT–PCR. Values are means ± SEM. Each value is the mean of three replicates. Data were analysed by unpaired *t*-tests. C. Senescent cells accumulate upon 5-aza-CdR treatment. 5-Aza-CdR treated KARPAS-299 and control cells were stained for β-galactosidase activity and counterstained with nuclear fast red. Note the abnormal enlarged shape of 5-aza-CdR treated cells.

This effect was also observed in ALK− MAC-2A cells, albeit less pronounced due to lower $p16^{INK4A}$ promoter methylation levels (Supplementary Fig. S2A). Quantitative RT–PCR showed induction of $p16^{INK4A}$ expression after 5-aza-CdR administration in KARPAS-299 cells and to a lower level in MAC-2A cells (Fig. 3B and Supplementary Fig. S2B). Re-expression of $p16^{INK4A}$ prompted us to investigate whether 5-aza-CdR treatment could induce senescence in KARPAS-299 cells, as $p16^{INK4A}$ is a key regulator of the Rb pathway and cellular senescence [37]. Indeed, 5-aza-CdR treated KARPAS-299 cells displayed a high percentage of senescent cells, as indicated by β-galactosidase staining, compared to untreated controls (Fig. 3C). Thus, 5-aza-CdR exerts pleiotropic effects on KARPAS-299 cells including apoptosis, cell cycle arrest and increased senescence associated β-galactosidase activity *in vitro*.

3.4. Global gene expression analysis of 5-aza-CdR treated ALK+ ALCL cells

In order to study the effects of inhibition of DNMTs and DNA methylation in ALK+ ALCL on global gene expression, we treated KARPAS-299 cells with 1 µM 5-aza-CdR and performed gene expression analysis using Affymetrix gene level arrays. After quality control, normalization and filtering, we identified 492 genes to be differentially expressed (unadjusted p-value < 0.05) after 5-aza-CdR treatment. Our 31 top differentially expressed genes after taking a cut-off of an adjusted p-value < 0.2 included nine cancer testis antigens, such as DAZ1, DAZL, CT45A6, and MAGE2B, which are normally not expressed in adult tissue except for testis, but are known to be activated upon DNMT inhibitor treatment [38]. Eight of the 31 genes are involved in cell migration and adhesion, five genes are associated with immune responses and four genes with cell migration and adhesion and immune responses (Fig. 4A and Supplementary Table 1). We independently confirmed increased expression of MAGE2B, MMP13, SPARC, TGFB1, TNFAIP2 and CXCL11 by qRT–PCR after 5-aza-CdR treatment (Fig. 4B).

Pathway analysis of all 492 genes (unadjusted p-value < 0.05) by using ingenuity pathway analysis (IPA) software revealed cancer as top associated "biological function". Further changes were detected for genes involved in cellular movement, inflammatory response, cell death and cellular growth and proliferation (Fig. 4C). Interestingly, the most affected transcription regulators included p53, which is in accordance with our observation that 5-aza-CdR leads to apoptosis and re-expression of epigenetically silenced tumor suppressors, and STAT3, which is an important down-stream mediator of ALK–induced signaling (Supplementary Table 2). We repeated the analysis with preselected genes including only genes that have been previously defined in response to 5-aza-CdR treatment to further validate our data [29,30]. Of these 725 preselected

genes 85 genes were differentially regulated (unadjusted p-value < 0.05) in KARPAS-299 cells after 5-aza-CdR treatment. After correction for multiple testing, eight genes remained significant (adjusted $p < 0.05$). Seven of these were found in our top 31 differentially regulated genes (Supplementary Table 3). In summary, our analysis detected deregulation of previous targets of 5-aza-CdR involved in apoptotic pathways, cellular growth and proliferation.

3.5. 5-Aza-CdR inhibits tumor growth of ALK+ cells in a murine xenograft model

To test the effects of 5-aza-CdR treatment on tumor growth and proliferation *in vivo*, we performed murine xenograft experiments employing different drug schedules. 1×10^6 ALK+ KARPAS-299 cells were subcutaneously injected into both flanks of SCID mice. In initial experiments, mice were treated with 2.5 mg/kg/mouse of 5-aza-CdR by intraperitoneal injection every day (treatment schedule Supplementary Fig. S3A). The time point of 5-aza-CdR administration after tumor injection significantly affected tumor growth. If 5-aza-CdR was administered for the first time 11 days after tumor inoculation, when tumor size already exceeded 1 cm^2, and then for a period of eight days, a slight but not statistically significant decrease in tumor weight was detected compared to control mice (Supplementary Fig. S3B). To optimize treatment outcome, we initiated treatment at an earlier stage and reduced the total amount of drug given. The animals were treated with 5-aza-CdR three days (two mice) or five days (three mice) after injection; thereafter treatment was continued every other day. Thereby, each mouse received five dosages of 5-aza-CdR in total. The control group contained two mice. As depicted in Fig. 5A, tumors from 5-aza-CdR treated mice were much smaller and tumor weight was significantly reduced in both treatment groups compared to the control group (Fig. 5B). Immunohistochemical staining for tumor proliferation by Ki-67-antibody revealed reduced Ki-67 expression in 5-aza-CdR treated tumors. Histology staining of 5-aza-CdR tumors showed large necrotic areas and increased apoptosis was detected by staining for caspase3 in FFPE sections of treated tumors (Fig. 5C).

FACS analysis revealed that $58\% \pm 5.1\%$ and $44.9\% \pm 7.0\%$ of tumor cells from 5-aza-CdR day 3 and 5-aza-CdR day 5 groups, respectively, were apoptotic, versus $29.5\% \pm 3.2\%$ in controls (Fig. 6A). DNMT1 protein was not detectable in protein extracts derived from 5-aza-CdR treated tumors as compared to controls, indicating a very efficient inhibition of DNMT1 by 5-aza-CdR incorporation into the tumor DNA (Fig. 6B). In accordance with these findings, all 5-aza-CdR treated tumors displayed demethylation at the $p16^{INK4A}$ promoter, which ranged from fully methylated in untreated to about 50% methylated in treated tumors, respectively (Fig. 6C and D). Therefore, we conclude that 5-aza-CdR shows high efficacy on ALCL xenografts *in vivo* and causes increased apoptosis and reduced proliferation of engrafted tumors.

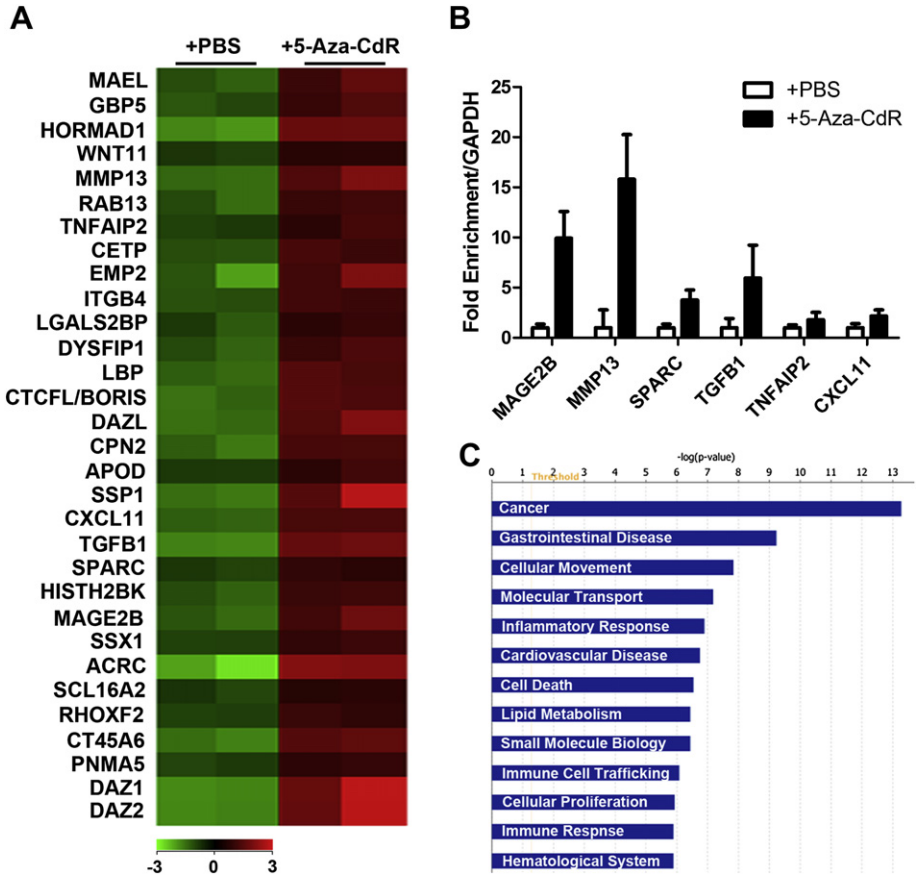

Fig. 4. Gene expression analysis of 5-aza-CdR treated KARPAS-299 cells. A. Heat map showing the top 31 differentially regulated genes after 5-aza-CdR treatment. Quality control, normalization, filtering and statistical analysis of array data was performed as described in materials and methods. The top 31 differentially expressed genes include cancer testis antigens, genes involved in cell adhesion and migration, and genes associated with immune response. B. qRT–PCR validation of six differentially expressed genes (MAGE2B, MMP13, SPARC, TGFB1, TNFAIP2 and CXCL11) confirms up-regulation after 5-aza-CdR treatment. C. Pathway analysis by IPA identifies cancer, cellular movement, inflammatory responses, cell death and cellular growth and differentiation as top "biological functions" affected by 5-aza-CdR.

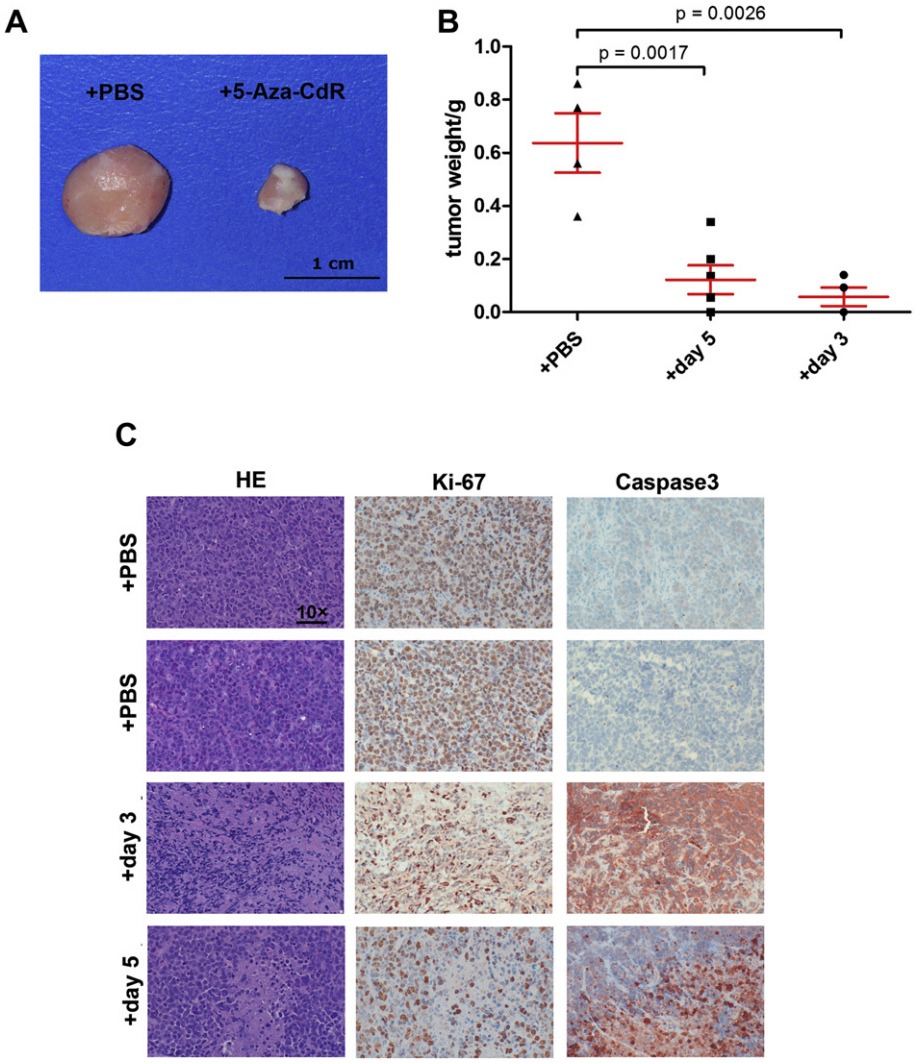

Fig. 5. 5-Aza-CdR inhibits ALCL cell proliferation in murine xenografts. A. 5-Aza-CdR treated mice develop no or smaller tumors compared to PBS treated controls. 1×10^6 ALK+ KARPAS-299 cells were subcutaneously injected into both flanks of SCID mice. Mice were treated with 2.5 mg/kg/mouse of 5-aza-CdR by intraperitoneal injection three days (two mice) or five days (three mice) after injection, respectively. Treatment was continued every other day and each mouse received five 5-aza-CdR treatments in total. The control group contained two mice. Representative 5-aza-CdR and control tumors are shown. B. Tumor weight of 5-aza-CdR samples is significantly decreased compared to controls. The aligned dot blots show means ± SEM. Tumor weights were analysed by one-way ANOVA ($p < 0.05$) followed by pair wise comparisons to the control group using unpaired *t*-tests. C. Immunohistochemical analysis of 5-aza-CdR tumors shows increased necrotic areas in hematoxylin and eosin (HE), decreased proliferation by Ki-67 staining and increased apoptosis by Caspase3 staining compared to PBS controls. Representative tumors of both treatment schedules and controls are shown.

4. Discussion

The DNMT inhibitor 5-aza-CdR is approved for the treatment of myelodysplastic syndrome and is tested in clinical trials for AML and CML, making it a promising therapeutic possibility for hematological malignancies [8,9,39,40]. In the current study, we observed a strong antineoplastic activity of 5-aza-CdR on anaplastic large cell lymphoma, a rare and aggressive CD30 positive lymphoma of T-cell origin [12]. ALCL cells displayed high DNMT1 expression, which is considered a sign for actively proliferating cells and a prerequisite for 5-aza-CdR incorporation into DNA. ALCL cells responded to drug treatment with significantly decreased cell proliferation, G1 arrest, increased apoptosis and loss of methylation. These effects were visible only after several days in culture, as would be expected for a mechanism involving passive DNA demethylation and no cytotoxicity. Notably, we observed an EC_{50} value of 5-aza-CdR for the ALK+ Karpas-299 cell line in the same range as those reported for four common AML cell lines (0.49 μM vs. 0.4–0.8 μM) [34]. 5-Aza-CdR plasma concentrations measured in clinical studies vary between 0.3 and 1.6 μM, indicating that 5-aza-CdR concentrations determined *in vitro* for successful ALCL proliferation inhibition could potentially be achieved in humans [41,42]. Our xenograft studies showed that the effects obtained *in vitro* can also be observed *in vivo* regarding tumor growth inhibition, induction of apoptosis, and demethylation of candidate genes. Early administration time points were critical for effective drug action, probably due to the high aggressivity of the tumors. In addition, possible inhibitory effects of 5-aza-CdR on blood vessel formation have been observed in different tumor models, which might in part be responsible for the pronounced effect on tumor cell growth in our xenograft model [43].

Global gene expression analysis revealed that main changes induced by 5-aza-CdR concerned genes related to cell death, which is in line with our finding that 5-aza-CdR leads to reduced cell proliferation and apoptosis. Changes were also observed for genes involved in cell adhesion and migration and in immune response.

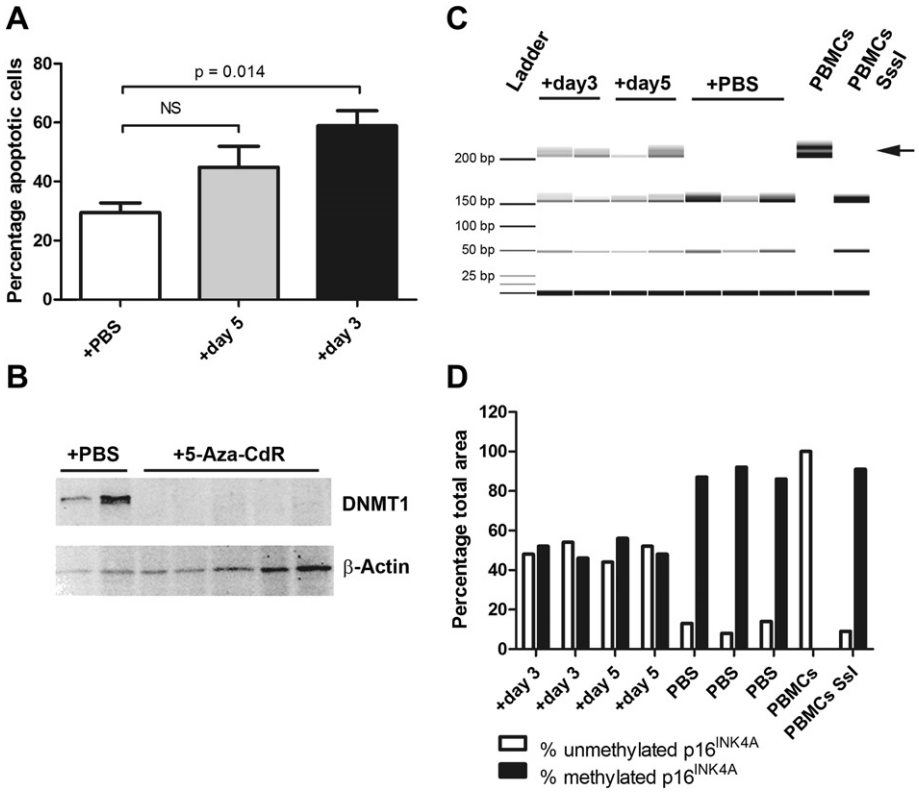

Fig. 6. 5-Aza-CdR treatment in vivo leads to inhibition of DNMT1 and apoptosis and results in demethylation of tumor suppressor p16INK4A. A. Cell cycle analysis shows that 5-aza-CdR treatment leads to increased apoptosis. Tumor samples were prepared for FACS analysis as described in the methods section and analyzed with a BD FACSCanto II flow cytometer using the BD FACS Diva Software. Values are means ± SEM. Each value is the mean of three replicates for control and 5-aza-CdR day 5 tumors and of two replicates for 5-aza-CdR day 3 tumors. B. DNMT1 is not detected in tumor protein extracts derived from 5-aza-CdR treated mice. Proteins were extracted from tumor tissue from two tumors treated with 5-aza-CdR starting on day 3 and three tumors treated with 5-aza-CdR on day 5 as described in materials and methods. DNMT1 protein levels were analysed by Western Blot. C. Analysis of the $p16^{INK4A}$ promotor region by COBRA shows demethylation after 5-aza-CdR treatment. DNA was extracted from tumor tissue, bisulfite converted and analysed by COBRA. Restriction fragments were analysed using the Agilent 2100 Bioanalyzer platform. Normal PBMCs and *in vitro* by M.SssI methylated PBMCs were used as unmethylated and methylated controls, respectively. Note the re-appearance of the unmethylated fragment in treated samples indicated by the arrow. D. The percentage of methylated fragments is significantly reduced in 5-aza-CdR treated tumors. Percentages of methylated and unmethylated fragments in relation to total peak areas in electropherograms were calculated with Agilent software as described in the methods section.

Our top de-regulated target TGFB1, which is a cytokine important for proliferation and differentiation of immune cells, was reported to be a marker for malignant transformation and drug sensitivity in melanoma cells [44]. Interestingly, its expression was observed to be low in ALK+ Karpas-299 compared to other ALK+ cell lines [45]. We also detected up-regulation of several cancer testis antigens such as MAGEB2, CT45A6, DAZL and BORIS/CTCFL, a finding that has regularly been reported for studies on DNA demethylation after 5-aza-CdR treatment [38,46]. Up-regulation of cancer testis antigens by DNA methylation inhibitors might represent a way to generate novel targets for cancer immunotherapy, as cancer testis antigens are not expressed in normal adult tissues except for testis or placenta [47].

Concerning the mechanism of action of 5-aza-CdR on tumor cells, the general hypothesis is that reversal of epigenetic gene silencing of tumor suppressors can contribute significantly to the proliferation inhibiting effects of the drug [4,48]. In our study, we observed demethylation and re-expression of the tumor suppressor $p16^{INK4A}$ (CDKN2A), which is involved in cell cycle G1 control by inhibiting cyclin-dependent kinase 4 (CDK4) and is epigenetically silenced in ALCL [19]. It has recently been shown that activation of the $p16^{INK4A}$/pRB pathway represents an alternative route to oncogene-induced senescence in ALK+ ALCL [37]. The presence of $p16^{INK4A}$ expressing cells was described in premalignant lesions of NPM-ALK transgenic mice rendering these cells senescent, whereas in the absence of $p16^{INK4A}$ tumors evolve rapidly. In line with this and our finding that the $p16^{INK4A}$ promoter is demethylated and re-expressed after 5-aza-CdR administration, we could also detect an increased number of senescent cells upon 5-aza-CdR treatment. Furthermore, in ALK + ALCL the fusion protein NPM-ALK has been implicated to be involved in epigenetic silencing of important tumor suppressors such as SHP-1, STAT5A and IL-2Rγ via its downstream target STAT3 [49–51]. Their re-expression leads to suppression of NPM-ALK expression and, subsequently, induction of apoptotic cell death. Therefore, it is tempting to speculate that 5-aza-CdR might exert part of its antineoplastic activity in ALK+ ALCL via demethylation of these tumor suppressor genes.

In addition, Zhang et al. showed that the transcription factor STAT3 can induce the expression of DNMT1 via miR-21, and vice versa inhibition of DNMT1 leads to suppression of STAT3 activation [24,51]. Considering that activated STAT3 is a key mediator of ALK induced downstream signaling events and is involved in the epigenetic silencing of tumor suppressors, inhibition of DNMT1 by 5-aza-CdR could have implications on the signaling pathways affected by STAT3. Our pathway analysis of the global gene expression data after 5-aza-CdR treatment listed STAT3 under the top transcriptional regulators, indicating that several STAT3 regulated proteins were affected by 5-aza-CdR. No relevant canonical pathway in STAT3 or ALK+ mediated signaling was detected to be de-regulated after inhibitor treatment, but possible changes in

STAT3 or ALK+ signaling might occur on protein level, as many ALK+ targets, such as STAT3, are posttranscriptionally activated via phosphorylation.

Currently, the efforts in therapeutic approaches of ALK+ and other kinase driven malignancies concentrate on inhibition of the kinase activity itself [52–54]. One prominent example is the tyrosine kinase inhibitor imatinib, which targets the bcr-abl oncoprotein in CML [55]. ALK specific inhibitors have been developed and are intensively tested in preclinical settings with promising results [56]. Despite good initial remission rates, targets of tyrosine kinase inhibitors tend to accumulate mutations, which lead to therapy resistance and tumor relapses of drug resistant cells [57,58]. We propose that our *in vitro* and *in vivo* data with 5-aza-CdR on ALCL suggest that an alternative option in these cases would be to target de-regulated epigenetic mechanisms such as promoter hypermethylation in tumor cells, and apply 5-aza-CdR either as single therapy or in combination with already established drugs.

Disclosure statement

All of the authors have nothing to declare as far as the conflict of interest is concerned.

Acknowledgments

We gratefully thank Susanne Heider for technical assistance with immunohistochemistry stainings. This work has been supported by the Austrian Science Fund (FWF) Elise Richter (V102-B12). MRH was supported by funds of the Oesterreichische Nationalbank (Anniversary Fund, project number 13061). KK was supported by FWF grant P19723.

Appendix A. Supplementary material

Supplementary data associated with this article can be found, in the online version, at http://dx.doi.org/10.1016/j.biochi.2012.05.029.

References

[1] R. Holliday, J.E. Pugh, DNA modification mechanisms and gene activity during development, Science 187 (1975) 226–232.
[2] P.A. Jones, S.B. Baylin, The fundamental role of epigenetic events in cancer, Nat. Rev. Genet. 3 (2002) 415–428.
[3] G. Egger, G. Liang, A. Aparicio, P.A. Jones, Epigenetics in human disease and prospects for epigenetic therapy, Nature 429 (2004) 457–463.
[4] C.B. Yoo, P.A. Jones, Epigenetic therapy of cancer: past, present and future, Nat. Rev. Drug Discov. 5 (2006) 37–50.
[5] D.V. Santi, C.E. Garrett, P.J. Barr, On the mechanism of inhibition of DNA–cytosine methyltransferases by cytosine analogs, Cell 33 (1983) 9–10.
[6] D.V. Santi, A. Norment, C.E. Garrett, Covalent bond formation between a DNA–cytosine methyltransferase and DNA containing 5-azacytosine, Proc. Natl. Acad. Sci. U S A 81 (1984) 6993–6997.
[7] H.M. Kantarjian, J.P. Issa, Decitabine dosing schedules, Semin. Hematol. 42 (2005) S17–S22.
[8] E. Kaminskas, A. Farrell, S. Abraham, A. Baird, L.S. Hsieh, S.L. Lee, J.K. Leighton, H. Patel, A. Rahman, R. Sridhara, Y.C. Wang, R. Pazdur, Approval summary: azacitidine for treatment of myelodysplastic syndrome subtypes, Clin. Cancer Res. 11 (2005) 3604–3608.
[9] J.P. Issa, G. Garcia-Manero, F.J. Giles, R. Mannari, D. Thomas, S. Faderl, E. Bayar, J. Lyons, C.S. Rosenfeld, J. Cortes, H.M. Kantarjian, Phase 1 study of low-dose prolonged exposure schedules of the hypomethylating agent 5-aza-2′-deoxycytidine (decitabine) in hematopoietic malignancies, Blood 103 (2004) 1635–1640.
[10] J.M. Scandura, G.J. Roboz, M. Moh, E. Morawa, F. Brenet, J.R. Bose, L. Villegas, U.S. Gergis, S.A. Mayer, C.M. Ippoliti, T.J. Curcio, E.K. Ritchie, E.J. Feldman, Phase 1 study of epigenetic priming with decitabine prior to standard induction chemotherapy for patients with AML, Blood 118 (2011) 1472–1480.
[11] Y. Boumber, J.P. Issa, Epigenetics in cancer: what's the future? Oncol. (Williston Park) 25 (2011) 220–226. 228.
[12] M.C. Kinney, R.A. Higgins, E.A. Medina, Anaplastic large cell lymphoma: twenty-five years of discovery, Arch. Pathol. Lab. Med. 135 (2011) 19–43.
[13] Y. Kaneko, G. Frizzera, S. Edamura, N. Maseki, M. Sakurai, Y. Komada, H. Tanaka, M. Sasaki, T. Suchi, et al., A novel translocation, t(2;5)(p23;q35), in childhood phagocytic large T-cell lymphoma mimicking malignant histiocytosis, Blood 73 (1989) 806–813.
[14] M.M. Le Beau, M.A. Bitter, R.A. Larson, L.A. Doane, E.D. Ellis, W.A. Franklin, C.M. Rubin, M.E. Kadin, J.W. Vardiman, The t(2;5)(p23;q35): a recurring chromosomal abnormality in Ki-1-positive anaplastic large cell lymphoma, Leukemia 3 (1989) 866–870.
[15] R. Rimokh, J.P. Magaud, F. Berger, J. Samarut, B. Coiffier, D. Germain, D.Y. Mason, A translocation involving a specific breakpoint (q35) on chromosome 5 is characteristic of anaplastic large cell lymphoma ('Ki-1 lymphoma'), Br. J. Haematol. 71 (1989) 31–36.
[16] H.M. Amin, R. Lai, Pathobiology of ALK+anaplastic large-cell lymphoma, Blood 110 (2007) 2259–2267.
[17] R. Chiarle, C. Voena, C. Ambrogio, R. Piva, G. Inghirami, The anaplastic lymphoma kinase in the pathogenesis of cancer, Nat. Rev. Cancer 8 (2008) 11–23.
[18] R.H. Palmer, E. Vernersson, C. Grabbe, B. Hallberg, Anaplastic lymphoma kinase: signalling in development and disease, Biochem. J. 420 (2009) 345–361.
[19] T. Nagasawa, Q. Zhang, P.N. Raghunath, H.Y. Wong, M. El-Salem, A. Szallasi, M. Marzec, P. Gimotty, A.H. Rook, E.C. Vonderheid, N. Odum, M.A. Wasik, Multi-gene epigenetic silencing of tumor suppressor genes in T-cell lymphoma cells; delayed expression of the p16 protein upon reversal of the silencing, Leuk. Res. 30 (2006) 303–312.
[20] C. Ambrogio, C. Martinengo, C. Voena, F. Tondat, L. Riera, P.F. di Celle, G. Inghirami, R. Chiarle, NPM-ALK oncogenic tyrosine kinase controls T-cell identity by transcriptional regulation and epigenetic silencing in lymphoma cells, Cancer Res. 69 (2009) 8611–8619.
[21] J.D. Khoury, G.Z. Rassidakis, L.J. Medeiros, H.M. Amin, R. Lai, Methylation of SHP1 gene and loss of SHP1 protein expression are frequent in systemic anaplastic large cell lymphoma, Blood 104 (2004) 1580–1581.
[22] Q. Zhang, H.Y. Wang, G. Bhutani, X. Liu, M. Paessler, J.W. Tobias, D. Baldwin, K. Swaminathan, M.C. Milone, M.A. Wasik, Lack of TNFalpha expression protects anaplastic lymphoma kinase-positive T-cell lymphoma (ALK+TCL) cells from apoptosis, Proc. Natl. Acad. Sci. U S A 106 (2009) 15843–15848.
[23] A. Akimzhanov, L. Krenacs, T. Schlegel, S. Klein-Hessling, E. Bagdi, E. Stelkovics, E. Kondo, S. Chuvpilo, P. Wilke, A. Avots, S. Gattenlohner, H.K. Muller-Hermelink, A. Palmetshofer, E. Serfling, Epigenetic changes and suppression of the nuclear factor of activated T cell 1 (NFATC1) promoter in human lymphomas with defects in immunoreceptor signaling, Am. J. Pathol. 172 (2008) 215–224.
[24] Q. Zhang, H.Y. Wang, A. Woetmann, P.N. Raghunath, N. Odum, M.A. Wasik, STAT3 induces transcription of the DNA methyltransferase 1 gene (DNMT1) in malignant T lymphocytes, Blood 108 (2006) 1058–1064.
[25] M.C. Le Deley, A. Reiter, D. Williams, G. Delsol, I. Oschlies, K. McCarthy, M. Zimmermann, L. Brugieres, Prognostic factors in childhood anaplastic large cell lymphoma: results of a large European intergroup study, Blood 111 (2008) 1560–1566.
[26] L. Gautier, L. Cope, B.M. Bolstad, R.A. Irizarry, Affy-analysis of Affymetrix GeneChip data at the probe level, Bioinformatics 20 (2004) 307–315.
[27] G.K. Smyth, Linear models and empirical bayes methods for assessing differential expression in microarray experiments, Stat. Appl. Genet. Mol. Biol. 3 (2004). Article3.
[28] R.C. Gentleman, V.J. Carey, D.M. Bates, B. Bolstad, M. Dettling, S. Dudoit, B. Ellis, L. Gautier, Y. Ge, J. Gentry, K. Hornik, T. Hothorn, W. Huber, S. Iacus, R. Irizarry, F. Leisch, C. Li, M. Maechler, A.J. Rossini, G. Sawitzki, C. Smith, G. Smyth, L. Tierney, J.Y. Yang, J. Zhang, Bioconductor: open software development for computational biology and bioinformatics, Genome Biol. 5 (2004) R80.
[29] D. Gius, H. Cui, C.M. Bradbury, J. Cook, D.K. Smart, S. Zhao, L. Young, S.A. Brandenburg, Y. Hu, K.S. Bisht, A.S. Ho, D. Mattson, L. Sun, P.J. Munson, E.Y. Chuang, J.B. Mitchell, A.P. Feinberg, Distinct effects on gene expression of chemical and genetic manipulation of the cancer epigenome revealed by a multimodality approach, Cancer Cell 6 (2004) 361–371.
[30] H. Caren, A. Djos, M. Nethander, R.M. Sjoberg, P. Kogner, C. Enstrom, S. Nilsson, T. Martinsson, Identification of epigenetically regulated genes that predict patient outcome in neuroblastoma, BMC Cancer 11 (2011) 66.
[31] R. Jaenisch, A. Bird, Epigenetic regulation of gene expression: how the genome integrates intrinsic and environmental signals, Nat. Genet. 33 (2003) 245–254.
[32] T. Chen, S. Hevi, F. Gay, N. Tsujimoto, T. He, B. Zhang, Y. Ueda, E. Li, Complete inactivation of DNMT1 leads to mitotic catastrophe in human cancer cells, Nat. Genet. 39 (2007) 391–396.
[33] G. Egger, S. Jeong, S.G. Escobar, C.C. Cortez, T.W. Li, Y. Saito, C.B. Yoo, P.A. Jones, G. Liang, Identification of DNMT1 (DNA methyltransferase 1) hypomorphs in somatic knockouts suggests an essential role for DNMT1 in cell survival, Proc. Natl. Acad. Sci. U S A 103 (2006) 14080–14085.
[34] P.W. Hollenbach, A.N. Nguyen, H. Brady, M. Williams, Y. Ning, N. Richard, L. Krushel, S.L. Aukerman, C. Heise, K.J. MacBeth, A comparison of azacitidine and decitabine activities in acute myeloid leukemia cell lines, PLoS One 5 (2010) e9001.
[35] P.A. Jones, S.M. Taylor, Cellular differentiation, cytidine analogs and DNA methylation, Cell 20 (1980) 85–93.

[36] S.M. Taylor, P.A. Jones, Multiple new phenotypes induced in 10T1/2 and 3T3 cells treated with 5-azacytidine, Cell 17 (1979) 771–779.
[37] P. Martinelli, P. Bonetti, C. Sironi, G. Pruneri, C. Fumagalli, P.R. Raviele, S. Volorio, S. Pileri, R. Chiarle, F.K. McDuff, B.K. Tusi, S.D. Turner, G. Inghirami, P.G. Pelicci, E. Colombo, The lymphoma-associated NPM-ALK oncogene elicits a p16INK4a/pRb-dependent tumor-suppressive pathway, Blood 117 (2011) 6617–6626.
[38] M. Almstedt, N. Blagitko-Dorfs, J. Duque-Afonso, J. Karbach, D. Pfeifer, E. Jager, M. Lubbert, The DNA demethylating agent 5-aza-2'-deoxycytidine induces expression of NY-ESO-1 and other cancer/testis antigens in myeloid leukemia cells, Leuk. Res. 34 (2010) 899–905.
[39] H.M. Kantarjian, S. O'Brien, J. Cortes, F.J. Giles, S. Faderl, J.P. Issa, G. Garcia-Manero, M.B. Rios, J. Shan, M. Andreeff, M. Keating, M. Talpaz, Results of decitabine (5-aza-2′deoxycytidine) therapy in 130 patients with chronic myelogenous leukemia, Cancer 98 (2003) 522–528.
[40] Y. Oki, H.M. Kantarjian, V. Gharibyan, D. Jones, S. O'Brien, S. Verstovsek, J. Cortes, G.M. Morris, G. Garcia-Manero, J.P. Issa, Phase II study of low-dose decitabine in combination with imatinib mesylate in patients with accelerated or myeloid blastic phase of chronic myelogenous leukemia, Cancer 109 (2007) 899–906.
[41] W. Blum, R.B. Klisovic, B. Hackanson, Z. Liu, S. Liu, H. Devine, T. Vukosavljevic, L. Huynh, G. Lozanski, C. Kefauver, C. Plass, S.M. Devine, N.A. Heerema, A. Murgo, K.K. Chan, M.R. Grever, J.C. Byrd, G. Marcucci, Phase I study of decitabine alone or in combination with valproic acid in acute myeloid leukemia, J. Clin. Oncol. 25 (2007) 3884–3891.
[42] A.F. Cashen, A.K. Shah, L. Todt, N. Fisher, J. DiPersio, Pharmacokinetics of decitabine administered as a 3-h infusion to patients with acute myeloid leukemia (AML) or myelodysplastic syndrome (MDS), Cancer Chemother. Pharmacol. 61 (2008) 759–766.
[43] D.M. Hellebrekers, K.W. Jair, E. Vire, S. Eguchi, N.T. Hoebers, M.F. Fraga, M. Esteller, F. Fuks, S.B. Baylin, M. van Engeland, A.W. Griffioen, Angiostatic activity of DNA methyltransferase inhibitors, Mol. Cancer Ther. 5 (2006) 467–475.
[44] R. Halaban, M. Krauthammer, M. Pelizzola, E. Cheng, D. Kovacs, M. Sznol, S. Ariyan, D. Narayan, A. Bacchiocchi, A. Molinaro, Y. Kluger, M. Deng, N. Tran, W. Zhang, M. Picardo, J.J. Enghild, Integrative analysis of epigenetic modulation in melanoma cell response to decitabine: clinical implications, PLoS One 4 (2009) e4563.
[45] M. Kasprzycka, M. Marzec, X. Liu, Q. Zhang, M.A. Wasik, Nucleophosmin/anaplastic lymphoma kinase (NPM/ALK) oncoprotein induces the T regulatory cell phenotype by activating STAT3, Proc. Natl. Acad. Sci. U S A 103 (2006) 9964–9969.
[46] D. Atanackovic, T. Luetkens, B. Kloth, G. Fuchs, Y. Cao, Y. Hildebrandt, S. Meyer, K. Bartels, H. Reinhard, N. Lajmi, S. Hegewisch-Becker, G. Schilling, U. Platzbecker, G. Kobbe, T. Schroeder, C. Bokemeyer, N. Kroger, Cancer-testis antigen expression and its epigenetic modulation in acute myeloid leukemia, Am. J. Hematol. 86 (2011) 918–922.
[47] R. Claus, M. Almstedt, M. Lubbert, Epigenetic treatment of hematopoietic malignancies: in vivo targets of demethylating agents, Semin. Oncol. 32 (2005) 511–520.
[48] C. Stresemann, F. Lyko, Modes of action of the DNA methyltransferase inhibitors azacytidine and decitabine, Int. J. Cancer 123 (2008) 8–13.
[49] Q. Zhang, H.Y. Wang, M. Marzec, P.N. Raghunath, T. Nagasawa, M.A. Wasik, STAT3- and DNA methyltransferase 1-mediated epigenetic silencing of SHP-1 tyrosine phosphatase tumor suppressor gene in malignant T lymphocytes, Proc. Natl. Acad. Sci. U S A 102 (2005) 6948–6953.
[50] Q. Zhang, H.Y. Wang, X. Liu, M.A. Wasik, STAT5A is epigenetically silenced by the tyrosine kinase NPM1-ALK and acts as a tumor suppressor by reciprocally inhibiting NPM1-ALK expression, Nat. Med. 13 (2007) 1341–1348.
[51] Q. Zhang, H.Y. Wang, X. Liu, G. Bhutani, K. Kantekure, M. Wasik, IL-2R common gamma-chain is epigenetically silenced by nucleophosphin-anaplastic lymphoma kinase (NPM-ALK) and acts as a tumor suppressor by targeting NPM-ALK, Proc. Natl. Acad. Sci. U S A 108 (2011) 11977–11982.
[52] M. Marzec, M. Kasprzycka, A. Ptasznik, P. Wlodarski, Q. Zhang, N. Odum, M.A. Wasik, Inhibition of ALK enzymatic activity in T-cell lymphoma cells induces apoptosis and suppresses proliferation and STAT3 phosphorylation independently of Jak3, Lab. Invest. 85 (2005) 1544–1554.
[53] W. Wan, M.S. Albom, L. Lu, M.R. Quail, N.C. Becknell, L.R. Weinberg, D.R. Reddy, B.P. Holskin, T.S. Angeles, T.L. Underiner, S.L. Meyer, R.L. Hudkins, B.D. Dorsey, M.A. Ator, B.A. Ruggeri, M. Cheng, Anaplastic lymphoma kinase activity is essential for the proliferation and survival of anaplastic large-cell lymphoma cells, Blood 107 (2006) 1617–1623.
[54] A.V. Galkin, J.S. Melnick, S. Kim, T.L. Hood, N. Li, L. Li, G. Xia, R. Steensma, G. Chopiuk, J. Jiang, Y. Wan, P. Ding, Y. Liu, F. Sun, P.G. Schultz, N.S. Gray, M. Warmuth, Identification of NVP-TAE684, a potent, selective, and efficacious inhibitor of NPM-ALK, Proc. Natl. Acad. Sci. U S A 104 (2007) 270–275.
[55] B.J. Druker, S. Tamura, E. Buchdunger, S. Ohno, G.M. Segal, S. Fanning, J. Zimmermann, N.B. Lydon, Effects of a selective inhibitor of the Abl tyrosine kinase on the growth of Bcr-Abl positive cells, Nat. Med. 2 (1996) 561–566.
[56] O. Merkel, F. Hamacher, E. Sifft, L. Kenner, R. Greil, Novel therapeutic options in anaplastic large cell lymphoma: molecular targets and immunological tools, Mol. Cancer Ther. 10 (2011) 1127–1136.
[57] S. Roychowdhury, M. Talpaz, Managing resistance in chronic myeloid leukemia, Blood Rev. 25 (2011) 279–290.
[58] A.M. Eiring, J.S. Khorashad, K. Morley, M.W. Deininger, Advances in the treatment of chronic myeloid leukemia, BMC Med. 9 (2011) 99.